Electronic Supporting Information

Solvatochromic behaviour of dithioether-functionalized triphenylamine ligands and their mechano-responsive Cu(I) coordination polymers

Dilip Pandey[a], Gopal Singh[a], Shivendu Mishra[a], Lydie Viau[b], Michael Knorr[b], Abhinav Raghuvanshi*[a]

Email: r.abhinav@iiti.ac.in

[a]*Department of Chemistry, Indian Institute of Technology, Indore, MP, India, 452020.*

[b]*Université de Franche-Comté, UMR CNRS 6213, Institut UTINAM, 16 Route de Gray, F-25000 Besançon, France.*

Table of contents

1. EXPERIMENTAL SECTION

1.1 General Information

All the chemicals were used as received from Sigma-Aldrich. All reactions were performed under nitrogen environment and checked by TLC using Merck 60 F254 pre-coated silica gel plate (0.25 mm thickness) and the products were revealed under a UV chamber. ^{1}H NMR and ^{13}C-NMR spectra were recorded on a Bruker 500 MHz NMR spectrometer (Bruker BioSpin AG, Faellanden, Switzerland), using $CDCl_3$ as solvent and known chemical shifts of residual proton signals of deuterated solvents (for ^{1}H-NMR) or carbon signals of deuterated solvents (for ^{13}C-NMR) as the internal standard. Liquid-chromatography mass spectrometer (LCMS) was determined with an Agilent Q-TOF 6510 mass spectrometer (Agilent Technologies, Santa Clara, CA, USA) using the direct injection method, and electrospray ionization (ESI) was used as an ionization technique. A Fluoromax-4p spectrofluorometer from Horiba JobinYvon was used to record the luminescence spectra of all the compounds (model: FM-100). OriginPro 8.1 was used to evaluate each luminescence emission spectrum. The luminescence spectra were adjusted for the instrument's spectrum sensitivity. The temperature was kept constant throughout each experiment at 25 °C.

1.2 Synthesis of CP1

Into a Schlenk tube under N_2, ligand $\mathbf{L_1}$ (0.050 g, 0.11 mmol) was dissolved in 5 mL acetonitrile and CuBr (0.032 g, 0.22 mmol) was separately dissolved in 3 ml acetonitrile. 1-2 mL methanol were also added in the CuBr solution to avoid the oxidation of copper(I). After that, the CuBr solution was added to the ligand solution and the reaction mixture was stirred for 6 h at room temperature. After 6 h, formation of a pink-colored precipitate was observed. Further workup was done in open air where the precipitate was filtered and washed with 5mL dichloromethane (2-3 times) and 5 ml MeCN to remove the unreacted reactants. The yield of **CP1** is 83% (54.5 mg). When 1:4 ratio of ligand $\mathbf{L_1}$ and CuBr was used upto 90% yield was observed. Anal. Calc. for $C_{24}H_{23}BrCuNS_4$ (597.14): C, 48.27; H, 3.88; N, 2.35; S, 21.48. Found: C, 48.35; H, 3.91; N, 2.37; S, 21.51%. IR (ATR): 1584, 1496, 1415, 1304, 1263, 1173, 748, 690, 610, 525, 452 cm^{-1}.

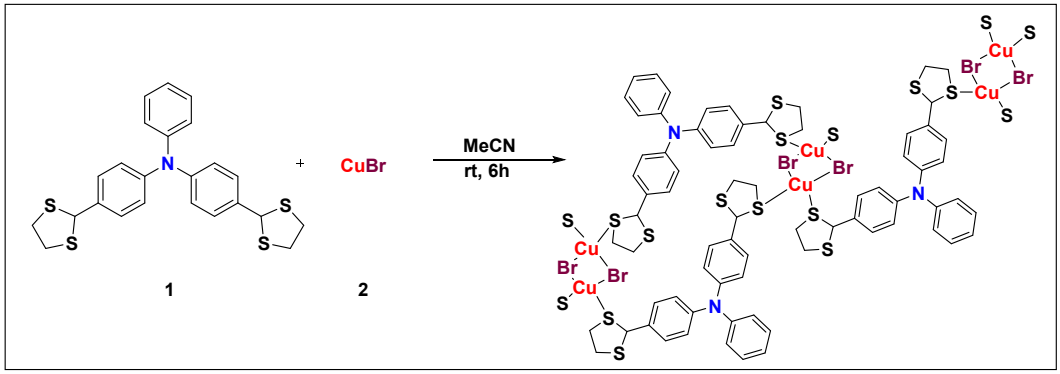

Scheme 1 Synthesis of coordination polymer **CP1**.

1.3 Synthesis of CP2

Into a Schlenk under N_2, ligand $\mathbf{L_1}$ (0.50 g, 0.11 mmol) was dissolved in 5 mL acetonitrile and CuCl (0.022 g, 0.22 mmol) was separately dissolved in 3 mL acetonitrile. Methanol (1-2 mL) was also added in the CuCl solution to avoid the oxidation of copper. After that, this CuCl solution was added to the ligand solution and the reaction mixture was stirred for 6 h at room temperature. After 6 h, a light pink-colored precipitate was observed, which was washed with 5mL dichloromethane (2-3 times) and 5 ml acetonitrile to remove the unreacted reactants. Further workup was done in open air where the precipitate was filtered and washed with 5mL dichloromethane (2-3 times) and 5 ml MeCN to remove the unreacted reactants. The yield of **CP2** is 79% (48.0 mg). When 1:4 ratio of ligand $\mathbf{L_1}$ and CuBr was used upto 82% yield was observed. Anal. Calc. for $C_{24}H_{23}ClCuNS_4$ (552.169): C, 52.16; H, 4.19; N, 2.53; S, 23.20. Found: C, 52.13; H, 4.14; N, 2.49; S, 23.17%. IR (ATR): 1586, 1479, 1415, 1300, 1263, 1167, 844, 749, 688, 530, 449 cm^{-1}.

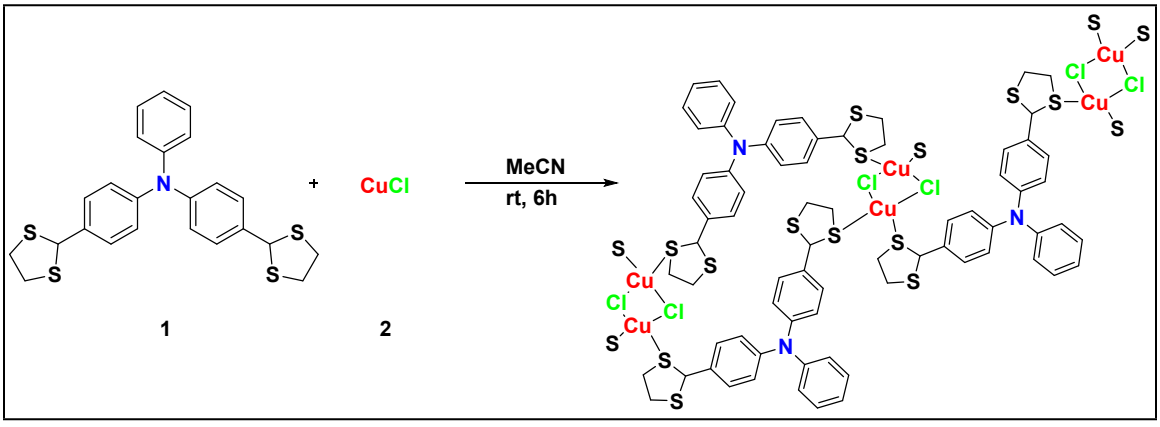

Scheme 2 Synthesis of coordination polymer **CP2**.

1.4 Synthesis of CP3

Into a Schlenk under N_2, ligand **L_2** (0.060 g, 0.124 mmol) was dissolved in 5 mL acetonitrile and CuBr (0.035 g, 0.248 mmol) was separately dissolved in 3 mL acetonitrile, methanol (1-2 mL) was also added in the CuBr solution to avoid the oxidation of copper. Then the CuBr solution was added to the ligand solution and the reaction mixture was stirred for 6 h at room temp. After 6 h, formation of a white precipitate was observed, which was filltered-off and washed with 5 mL dichloromethane (2-3 times). The yields of **CP3** is 69% (41.1 mg). Further workup was done in open air where the precipitate was filtered and washed with 5mL dichloromethane (2-3 times) and 5 ml MeCN to remove the unreacted reactants. The yield of **CP3** is 69% (41.1 mg). When 1:4 ratio of ligand **L_1** and CuBr was used upto 74% yield was observed. Anal. Calc. for $C_{26}H_{27}BrCuNS_4$ (625.19): C, 49.95; H, 4.35; N, 2.24; S, 20.51. Found: C, 49.92; H, 4.31; N, 2.19; S, 20.47%. IR (ATR): 1588, 1491, 1413, 1275, 1171, 754, 678, 610, 528, 452 cm^{-1}.

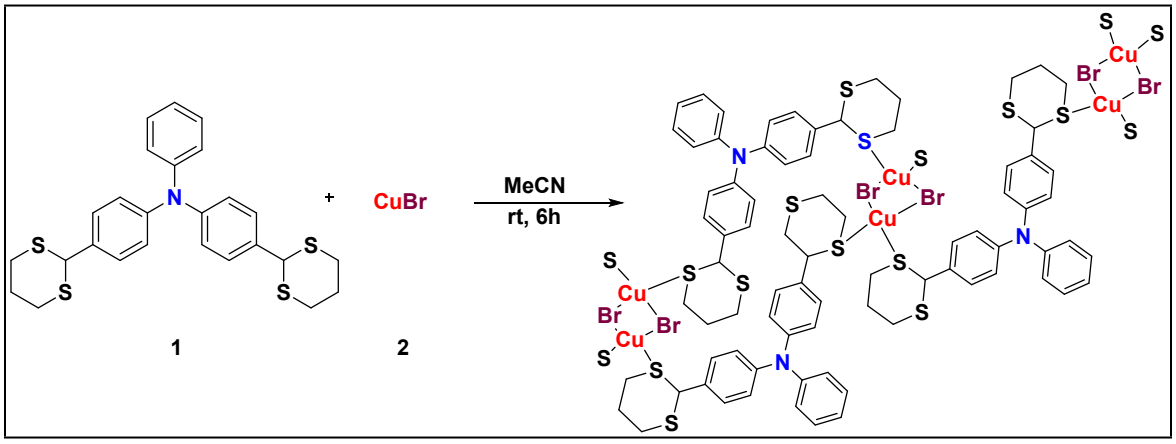

Scheme 3 Synthesis of coordination polymer **CP3**.

1.5 Synthesis of CP4

Into a Schlenk under N_2, ligand **L_2** (0.050 g, 0.103 mmol) was dissolved in 5 mL acetonitrile and CuCl (0.020 g, 0.206 mmol) was separately dissolved in 3 mL acetonitrile, methanol (1-2 mL) was also added in the CuCl solution to avoid the oxidation of copper. After that, this CuCl solution was added to the ligand solution and the reaction mixture was stirred for 6 h at room temperature. After

6 h, an off-white-colored precipitate was observed, that was washed with 5mL dichloromethane (2-3 times) The yield of **CP4** is 52% (25.7 mg). Further workup was done in open air where the precipitate was filtered and washed with 5mL dichloromethane (2-3 times) and 5 ml MeCN to remove the unreacted reactants. The yield of **CP4** is 52% (25.7 mg). When 1:4 ratio of ligand $\mathbf{L_1}$ and CuBr was used upto 55% yield was observed. Anal. Calc. for $C_{26}H_{27}ClCuNS_4$ (580.74): C, 53.77; H, 4.69; N, 2.41; S, 22.08. Found: C, 53.73; H, 4.67; N, 2.39; S, 22.04%. IR (ATR): 1590, 1506, 1323, 1271, 1167, 825, 762, 696, 513, cm^{-1}.

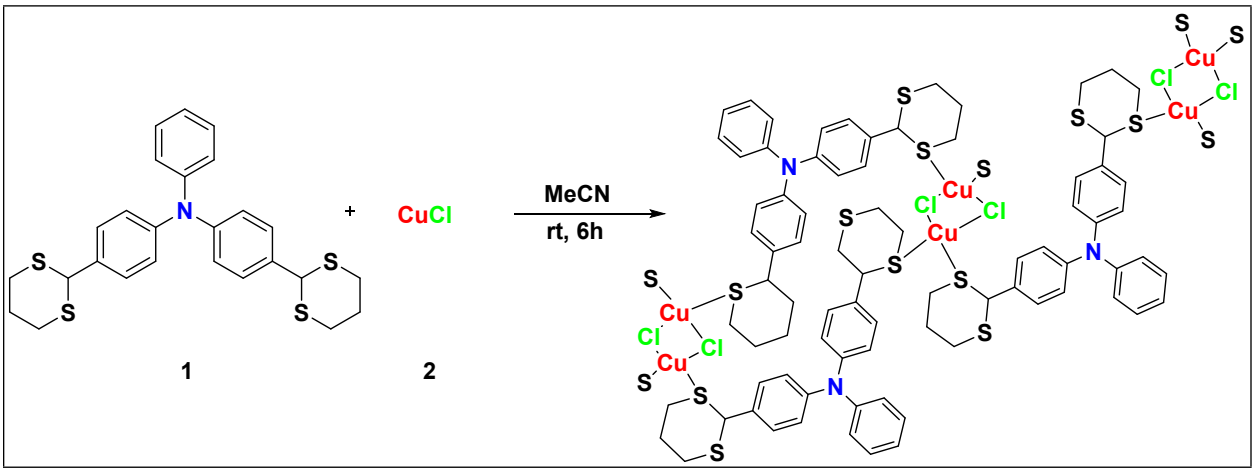

Scheme 4 Synthesis of coordination polymer **CP4**.

2. ^{1}H NMR spectra of the ligands

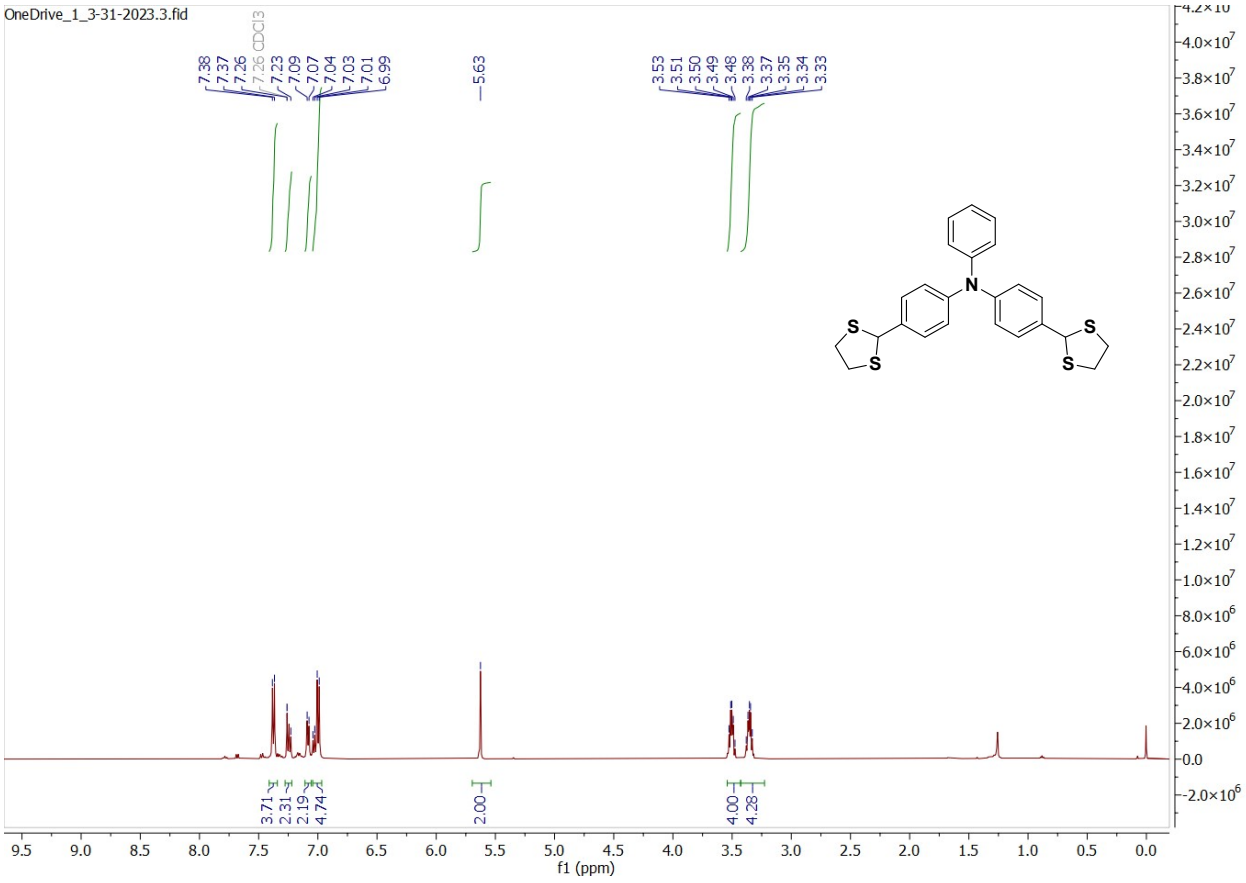

Fig. S1.1 ^{1}H NMR spectrum of $\mathbf{L_1}$ in $CDCl_3$.

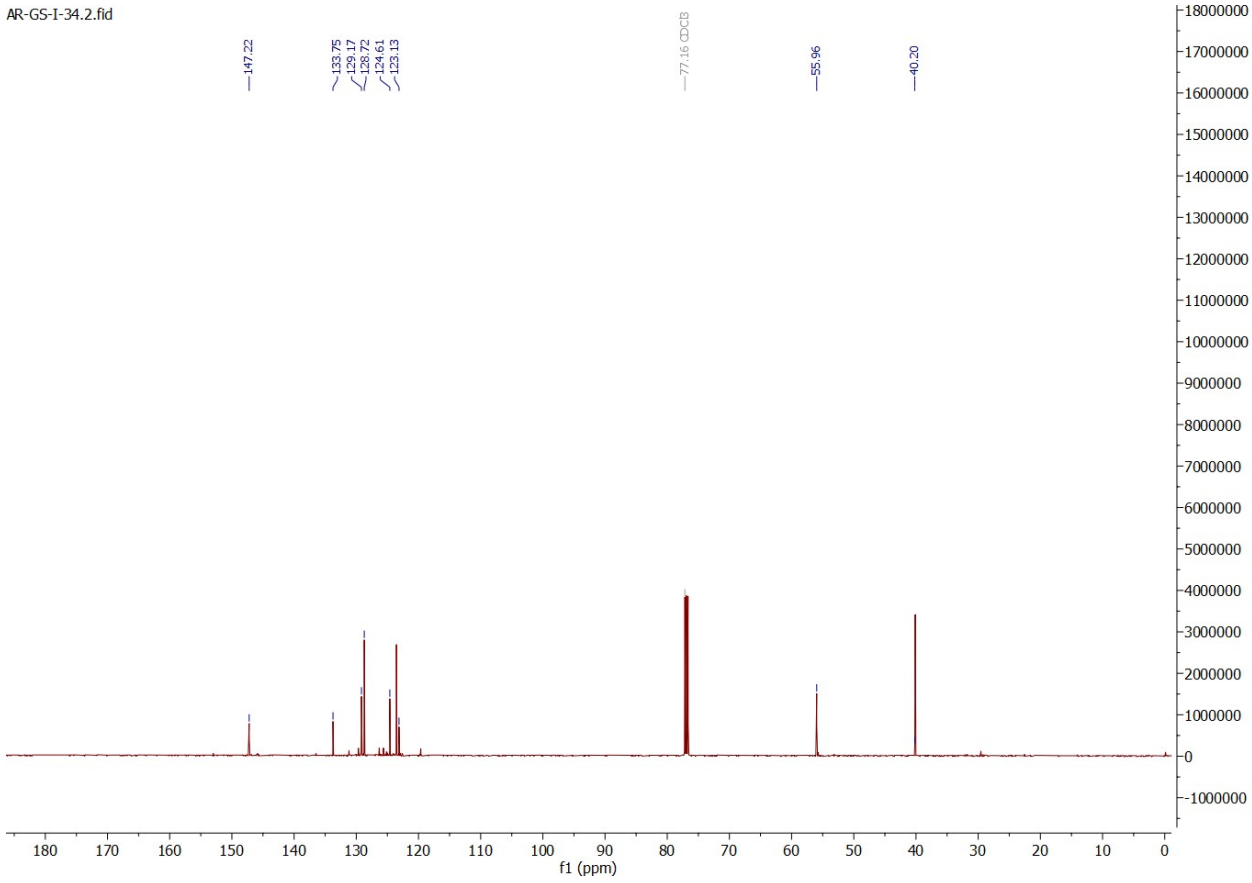

Fig. S1.2 ^{13}C NMR spectrum of $\mathbf{L_1}$ in $CDCl_3$.

.

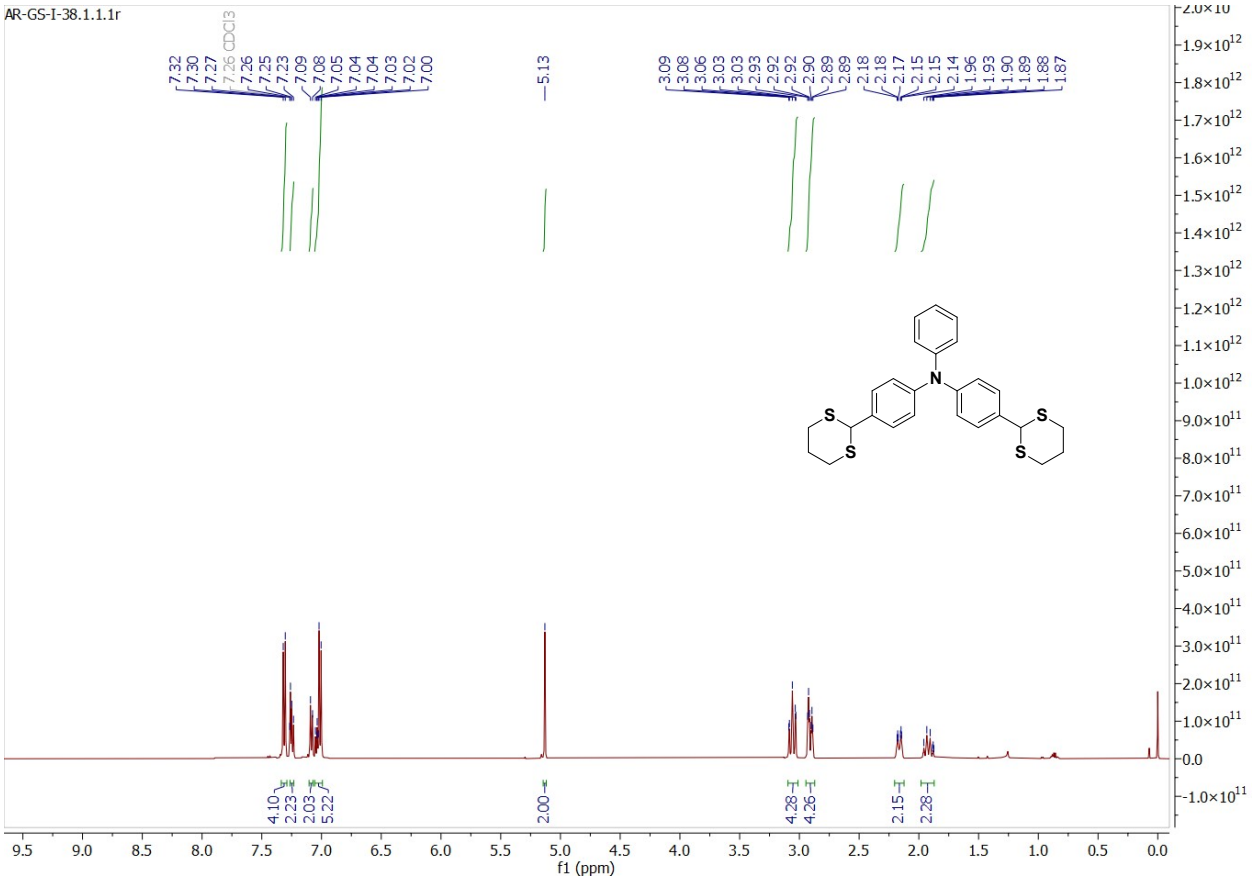

Fig. S2.1 ^{1}H NMR spectrum of $\mathbf{L_2}$ in $CDCl_3$.

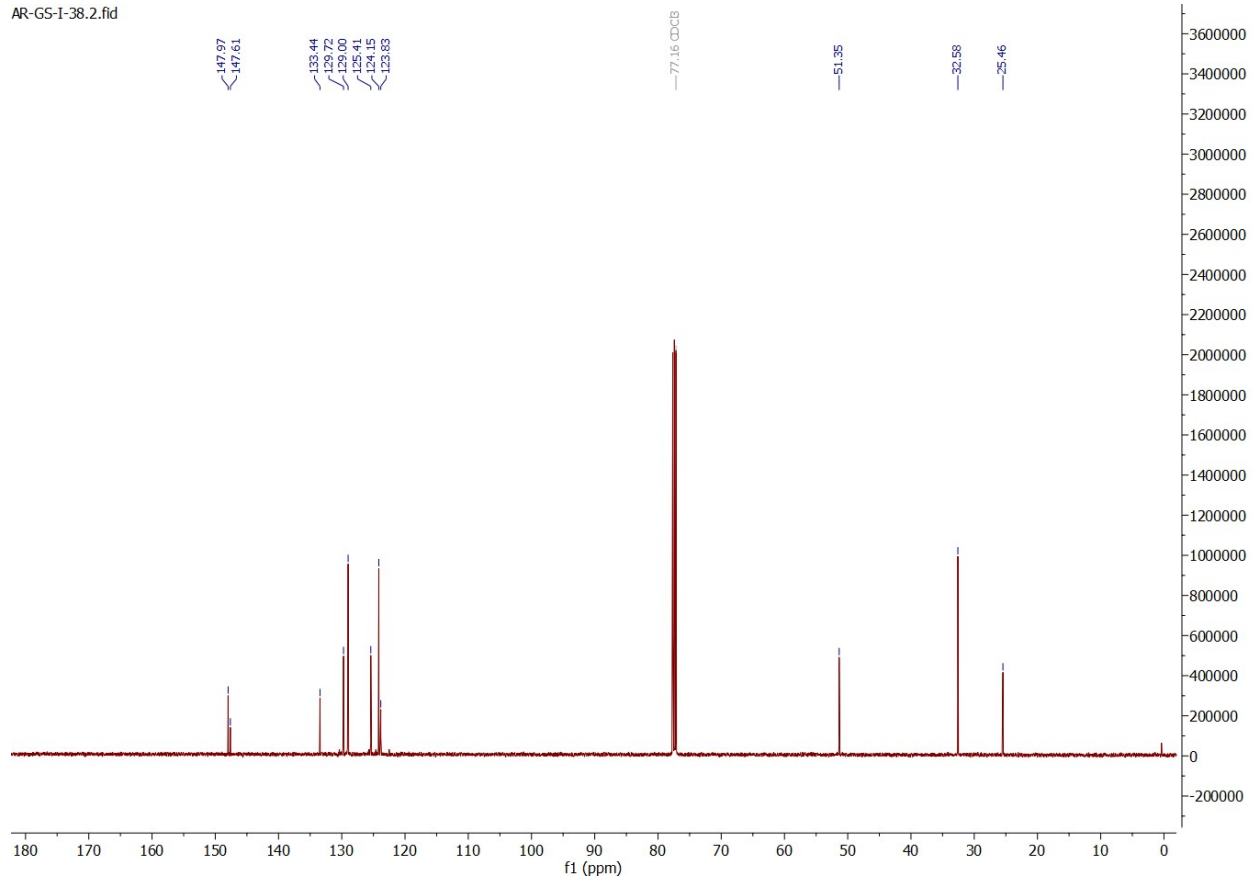

Fig. S2.2 ^{13}C NMR spectrum of $\mathbf{L_2}$ in $CDCl_3$.

3. Crystallographic details:

Single crystals suitable for single crystal X-ray crystallography were obtained by dissolving the solid samples in boiling acetonitrile and leaving it for few days at room temperature. Single crystal X-ray structural studies of crystals were performed on a CCDAgilent Technologies (Oxford Diffraction) SUPER NOVA diffractometer. Data for both the compounds were collected at 293 K

using a graphite-monochromated MoKα radiation (λα =0.71073 Å). The strategy for the data collection was evaluated by using the CrysAlisPro CCD software.8 The data were collected by the standard 'phi-omega scan techniques and were scaled and reduced using CrysAlisPro RED software. Using Olex2,[1] the structure was solved with the SHELXT structure solution program using Intrinsic Phasing and refined with the SHELXL[2] refinement package using Least Squares minimization.

Table S1. Crystallographic data of **CP1**, **CP2**, and ligand **L_2**

Compound	**L_2**	**CP1**	**CP2**
CCDC No	**2242123**	**2242124**	**2242127**
Formula	$C_{26}H_{27}NS_4$	$C_{24}H_{23}BrCuNS_4$	$C_{24}H_{23}ClCuNS_4$
Formula weight	481.72	597.12	552.66
Wavelength (Å)	0.71073	0.71073	0.71073
Crystal system	monoclinic	triclinic	triclinic
Space group	$P2_1/c$	P-1	P-1
a/Å	11.4918(6)	9.1864(5)	9.1410(5)
b/Å	19.6484(8)	10.4799(10)	10.4411(9)
c/Å	11.7522(7)	13.0998(10)	13.0328(8)
α/°	90	99.642(7)	100.066(6)
β/°	111.656(6)	103.110(5)	103.938(5)
γ/°	90	97.023(6)	95.714(6)
V/ Å³	2466.3(2)	1193.94(16)	1175.54(14)
Z	4	2	2
ρ_{calcd} (g/cm³)	1.297	1.661	1.561
Temperature/K	293.00	293.00	293.00
GOF	1.049	1.005	0.982
2θ range for data collection	7.016 to 49.996	6.28 to 49.992	6.35 to 49.998
Reflections collected	12620	9205	8170
Independent reflections	4189 [R_{int} = 0.0386]	4203 [R_{int} = 0.0747]	4094 [R_{int} = 0.1140]
Completeness to θ = 25.242	99.7	99.7	98.8
Final R indices [I>2σ(I)]	R_1 = 0.0485, wR_2 = 0.1138	R_1=0.0491, wR_2 =0.1206	R_1=0.0640, wR_2 = 0.1603
Final R indices	R_1 = 0.0635,	R_1= 0.0673,	R_1 = 0.1045,

[all data]	$wR_2 = 0.1229$	$wR_2 = 0.1294$	$wR_2 = 0.1927$
Largest diff. peak/hole/ eÅ^{-3}	0.36/-0.34	0.84/-0.73	0.69/-0.64

Table S2. Crystallographic data of **CP3**, and **CP4**

Compound	**CP3**	**CP4**
CCDC No.	**2242128**	**2242129**
Formula	$C_{26}H_{27}BrCuNS_4$	$C_{26}H_{27}ClCuNS_4$
Formula Weight	625.17	580.71
Wavelength	0.71073 Å	0.71073 Å
Crystal System	monoclinic	monoclinic
Space group	$P2_1/n$	$P2_1/n$
a/Å	10.1179(4)	10.1508(3)
b/ Å	9.9871(4)	10.0144(3)
c/ Å	26.3324(8)	25.8556(6)
α /°	90	90
β/°	97.071(3)	96.520(2)
γ/°	90	90
V/ Å^3	2640.61(17)	2611.33(13)
Z	4	4
ρ_{calcd} (g/cm^3)	1.573	1.477
Temperature/K	293.00	293.00
GOF	1.058	1.093
2θ range for data collection	6.09 to 49.998	5.824 to 49.994
Reflections collected	28346	18333
Independent reflections	4620 [R_{int} =0.0660]	4573 [R_{int} = 0.0554]
Completeness to θ=25.242	99.7	99.9
Final R indices [I>2σ(I)]	$R_1 = 0.0498$, $wR_2 = 0.1221$	$R_1 = 0.0600$, $wR_2 = 0.1643$

Final R indices [all data]	$R_1 = 0.0733$, $wR_2 = 0.1341$	$R_1 = 0.0923$, $wR_2 = 0.1843$
Largest diff. peak/hole/ e Å^{-3}	0.58/-0.71	0.81/-0.68

Table S3. Selected bond lengths (Å) for **CP1**-**CP4**.

Compounds	Average Cu−Cu	Average Cu−X	Average Cu−S
CP1	2.97	2.46	2.29
CP2	2.92	2.35	2.28
CP3	2.91	2.47	2.36
CP4	2.92	2.35	2.35

Table S4. Selected bond angles (°) for **CP1**-**CP4**.

Compounds	Average Cu−X−Cu	Average S−Cu−X	Average S−Cu−S
CP1	74.18	107.31	110.40
CP2	76.65	113.21	111.49
CP3	71.67	107.66	111.62
CP4	75.93	112.50	111.46

Table S5. The dihedral angle between the planes of different phenyl rings (**Ph_S – substituted phenyl and Ph_f – free phenyl)**.

Compounds	$Ph_S - Ph_f$	$Ph_S - Ph_S$	$Ph_S - Ph_f$

CP1	85.45	86.60	55.95
CP2	84.06	85.15	57.14
CP3	81.88	88.35	44.82
CP4	81.57	88.34	44.28

3.1. Crystal structures:

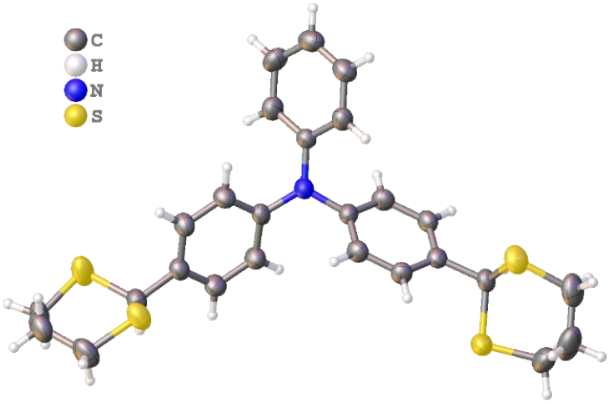

Fig. S3 Molecular structure of $\mathbf{L_2}$.

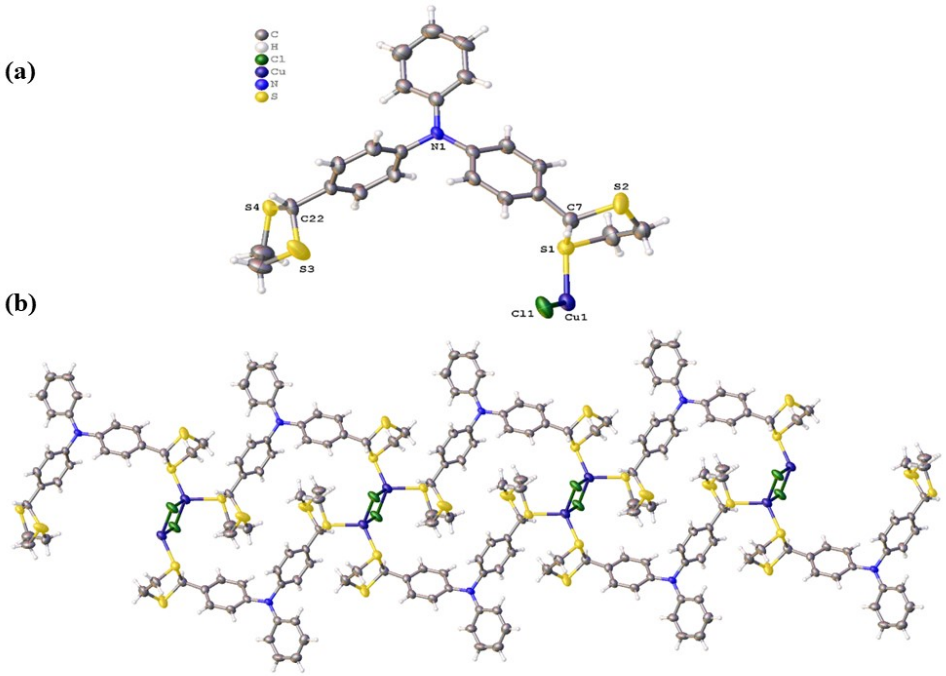

Fig. S4 (a) individual motif of **CP2 (b)** View of the 1D ribbon of $[\{Cu(\mu_2\text{-}Cl)_2Cu\}(\mu_2\text{-}\mathbf{L_1})]_n$ (**CP2**) running along the *a* axis. Symmetry transformations used to generate equivalent atoms: *[1]-X,1-Y,2-Z; [2]+X,+Y,1+Z; [1]-X,1-Y,2-Z; [2]+X,+Y,1+Z; [3]+X,+Y,-1+Z; [1]+X,+Y,-1+Z.*

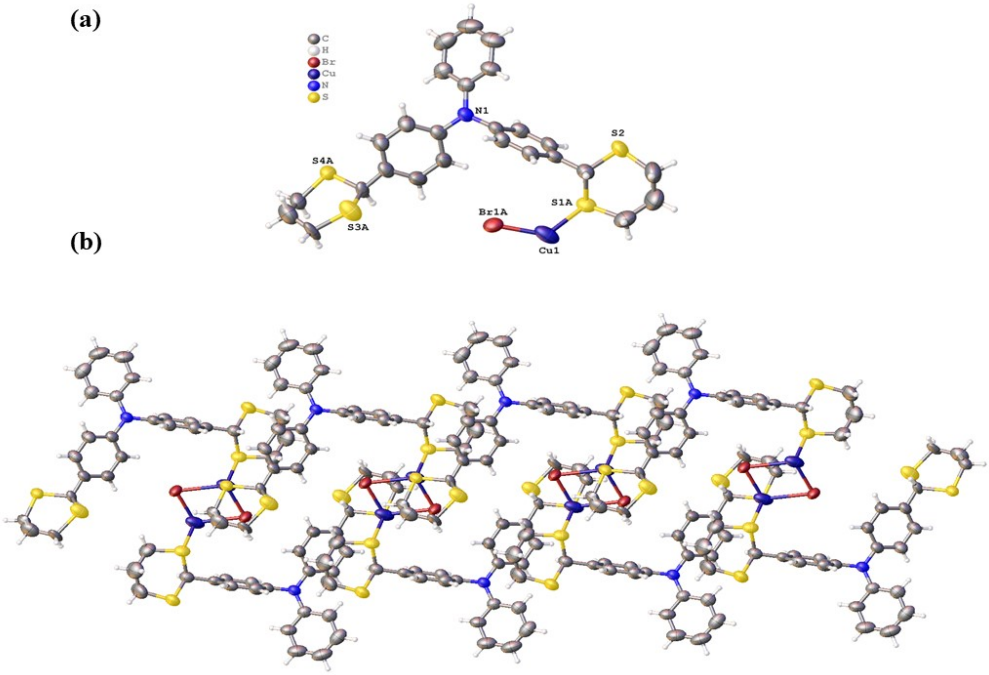

Fig. S5 (a) individual motif of **CP3 (b)** View of the 1D ribbon of $[\{Cu(\mu_2\text{-}Br)_2Cu\}(\mu_2\text{-}\mathbf{L_2})]_n$ (**CP3**) running along the *a* axis. Symmetry transformations used to generate equivalent atoms: *[1]1-X,1-Y,1-Z; [2]1+X,+Y,+Z; [1]1-X,1-Y,1-Z; [2]1+X,+Y,+Z; [3]-1+X,+Y,+Z; [1]-1+X,+Y,+Z.*

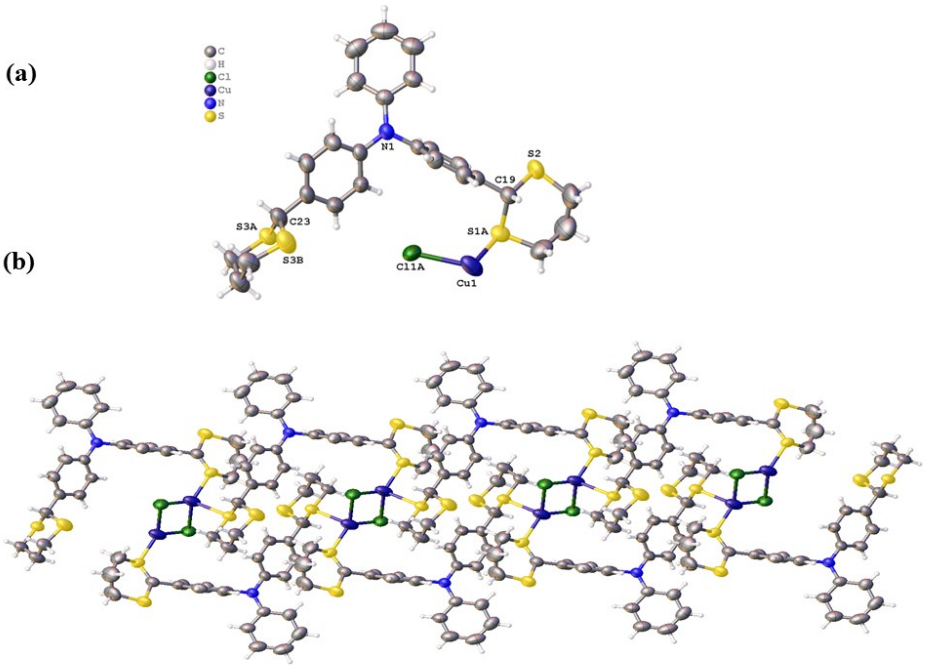

Fig. S6 (a) individual motif of **CP4 (b)** View of the 1D ribbon of $[\{Cu(\mu_2\text{-}Cl)_2Cu\}(\mu_2\text{-}\mathbf{L_2})]_n$ (**CP4**) running along the *a* axis. Symmetry transformations used to generate equivalent atoms: *[1]1-X,1-Y,1-Z; [2]1+X,+Y,+Z; [1]1-X,1-Y,1-Z; [2]1+X,+Y,+Z; [3]-1+X,+Y,+Z; [1]-1+X,+Y,+Z.*

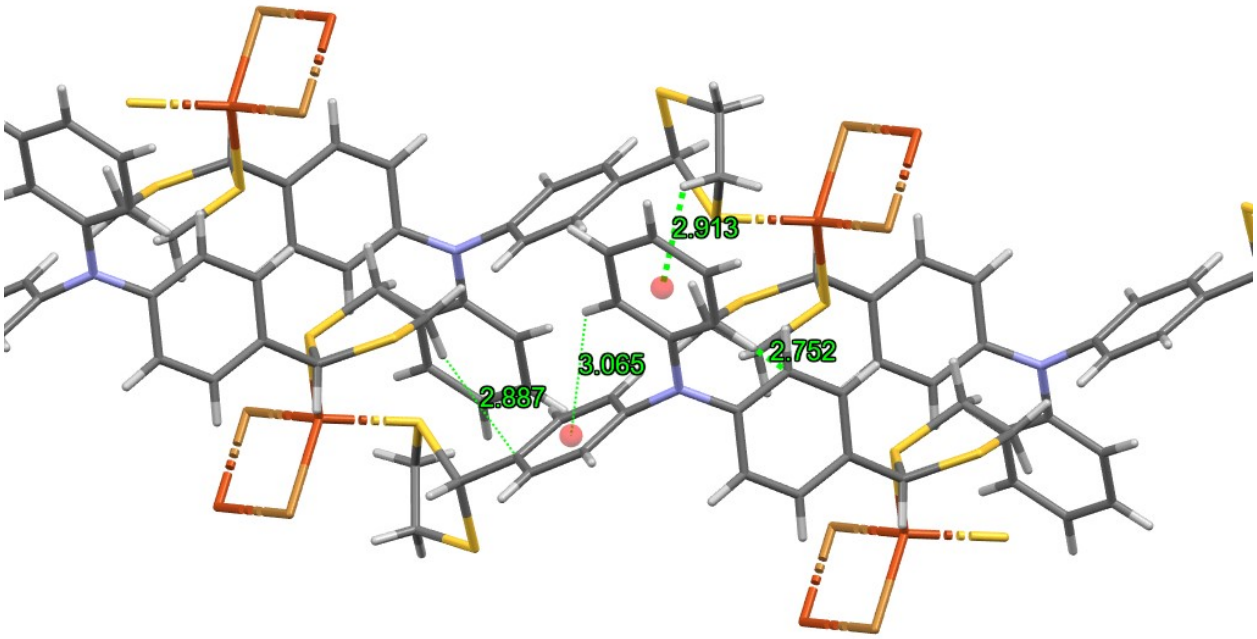

Fig. S7 Molecular packing of **CP1** indicating inter- and intramolecular C–H···π interactions. Symmetry transformations used to generate equivalent atoms: *[1]-X,1-Y,1-Z; [2]+X,+Y,1+Z [1]+X,+Y,-1+Z [1]+X,+Y,-1+Z [1]+X,+Y,-1+Z [1]+X,+Y,-1+Z*

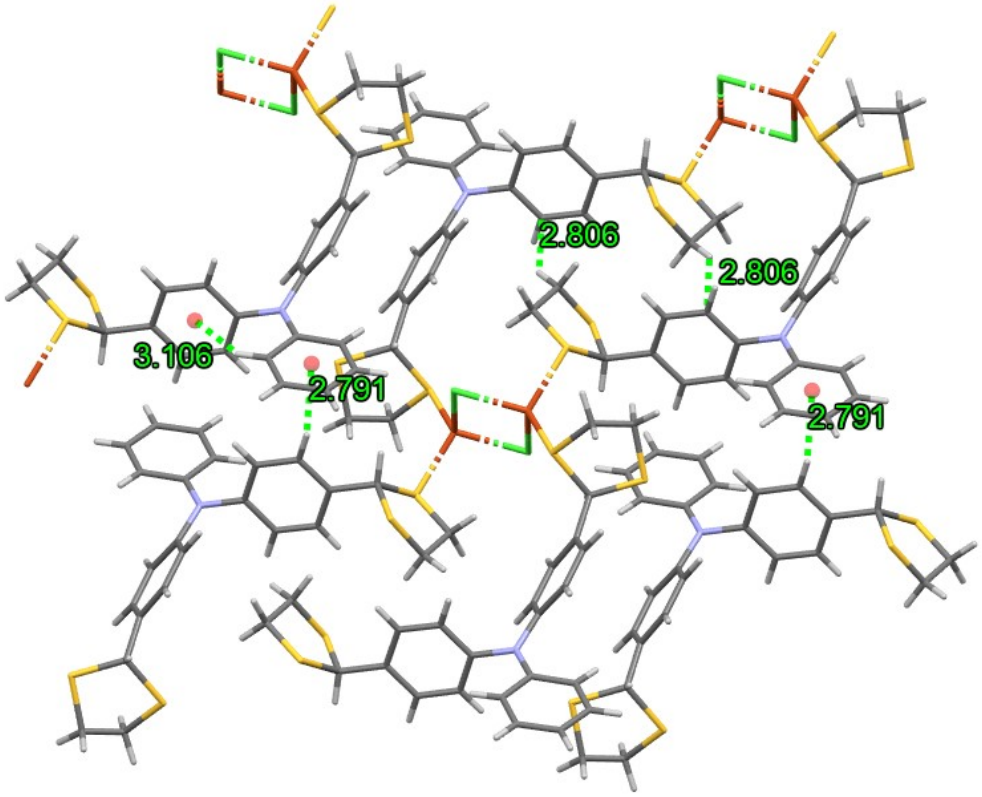

Fig. S8 Molecular packing of **CP2** with C–H···π interactions. Symmetry transformations used to generate equivalent atoms: *[1]-X,1-Y,2-Z; [2]+X,+Y,1+Z ; [1]-X,1-Y,2-Z; [2]+X,+Y,1+Z; [3]+X,+Y,-1+Z [1]+X,+Y,-1+Z*

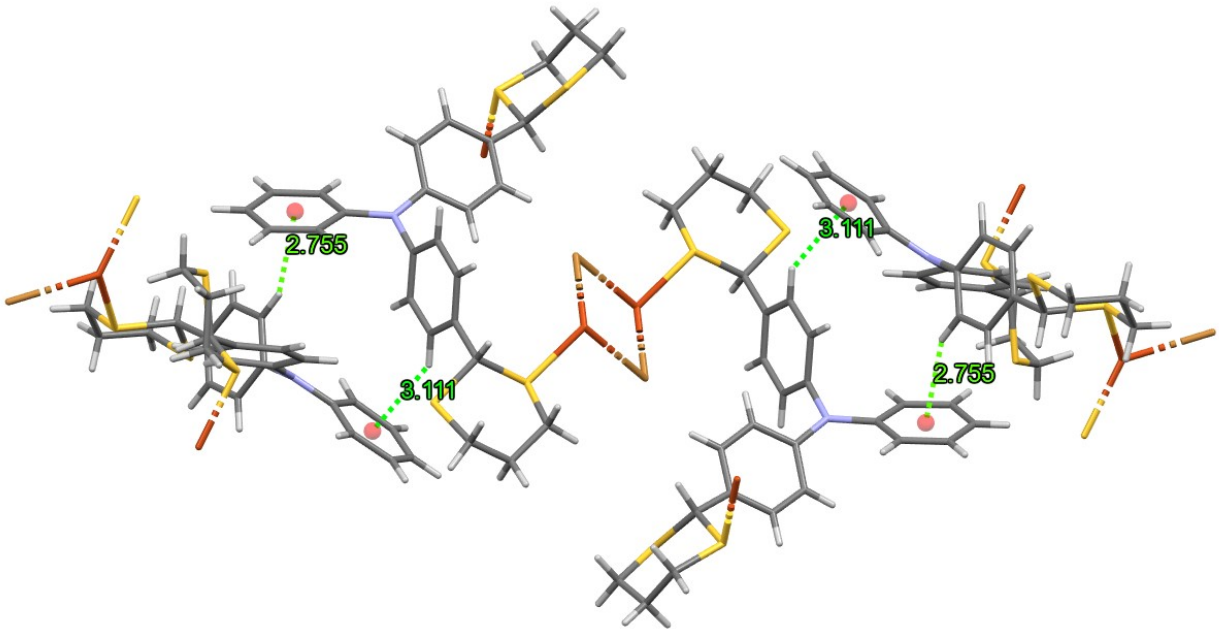

Fig. S9 Molecular packing of **CP3** with C–H···π interactions. Symmetry transformations used to generate equivalent atoms: [1]*1-X,1-Y,1-Z;* [2]*1+X,+Y,+Z ;* [1]*1-X,1-Y,1-Z;* [2]*1+X,+Y,+Z;* [3]*-1+X,+Y,+Z ;* [1]*-1+X,+Y,+Z*

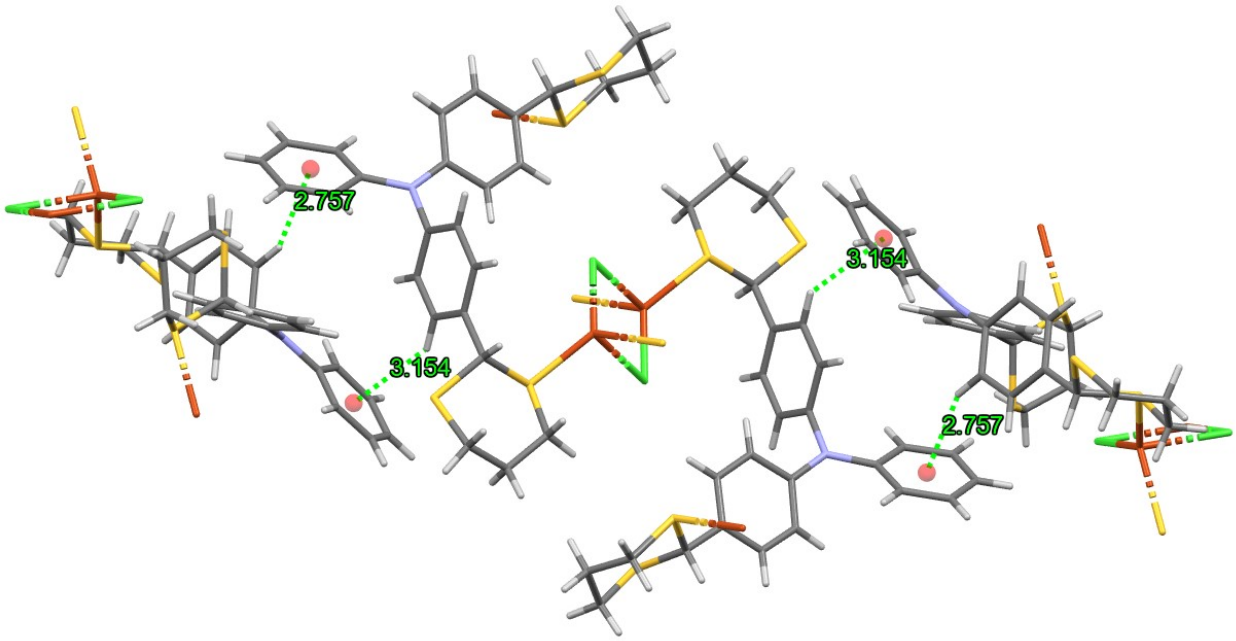

Fig. S10 Molecular packing of **CP4** with C–H···π interactions. Symmetry transformations used to generate equivalent atoms: *[1]1-X,1-Y,1-Z; [2]1+X,+Y,+Z ; [1]1-X,1-Y,1-Z; [2]1+X,+Y,+Z; [3]-1+X,+Y,+Z ; [1]-1+X,+Y,+Z*.

3.2. Dimensions of the 32-membered macrocyclic rings occurring in CP1-CP4:

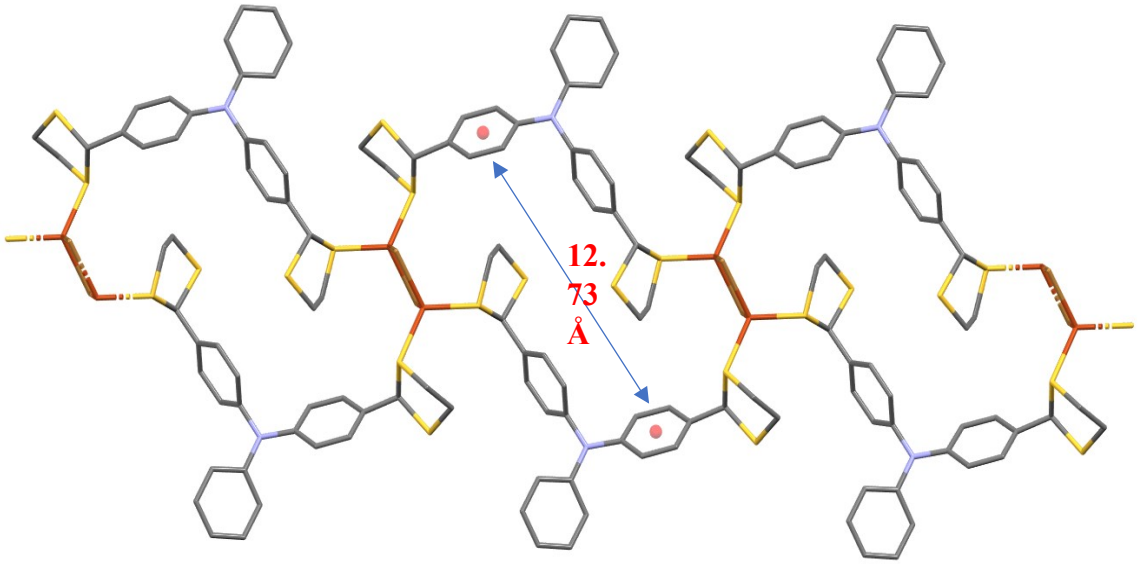

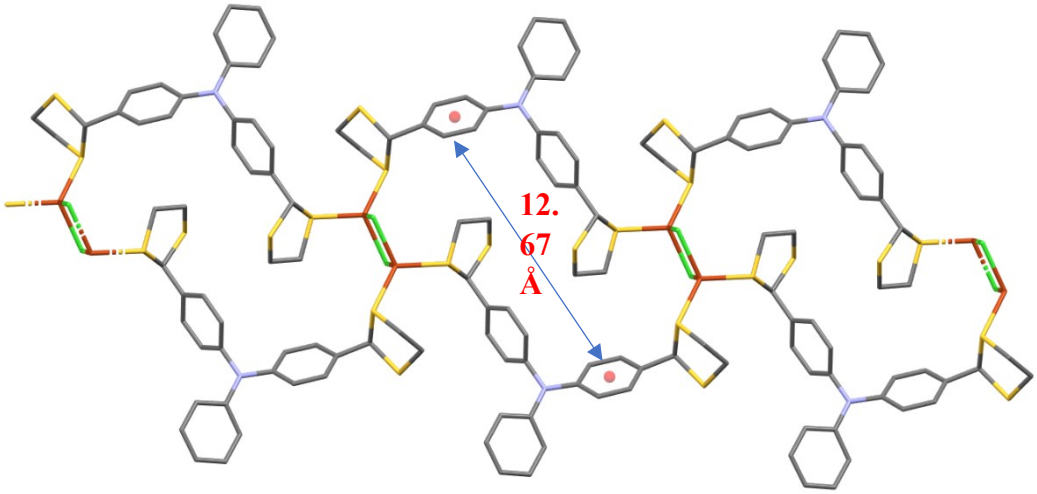

Fig. S11 Macrocyclic ring of **CP1**.

Fig. S12 Macrocyclic ring of **CP2**.

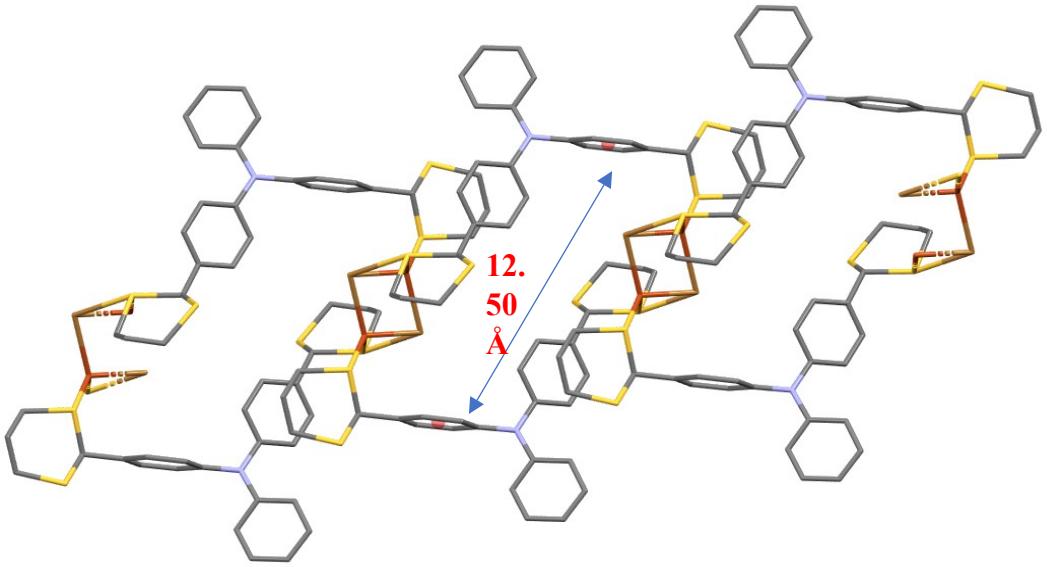

Fig. S13 Macrocyclic ring of **CP3**.

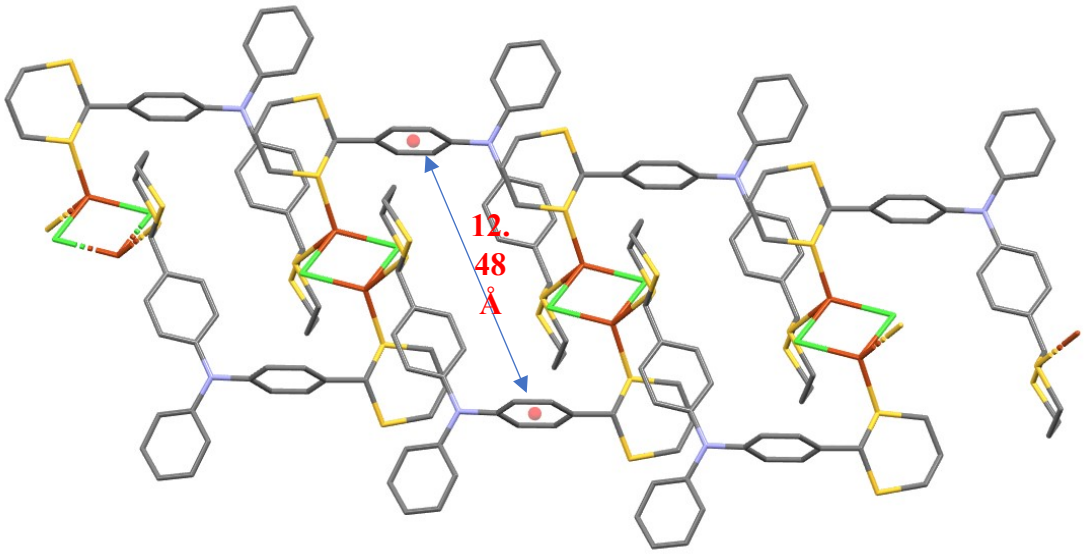

Fig. S14 Macrocyclic ring of **CP4**.

4. Photoluminescent properties of ligands

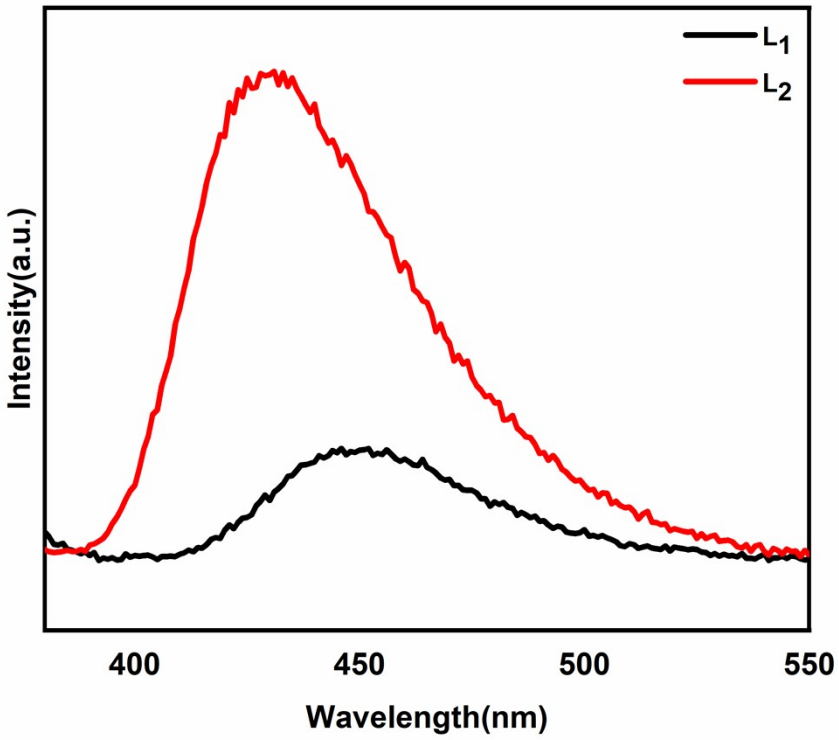

Fig. S15 Room temperature emission spectra of $\mathbf{L_1}$ and $\mathbf{L_2}$ upon excitation at 365 nm.

5. Powder X-ray diffraction (PXRD) pattern of CPs: Powder X-ray diffraction (PXRD) studies were performed at room temperature in air to confirm the CPs' bulk identity. We may infer that the bulk material and the crystals are homogeneous since the experimental PXRD patterns correlate well with the simulated data generated from X-ray single-crystal data. Different crystal orientations in the powder samples account for the discrepancy reflection intensities seen between the simulated and observed patterns.

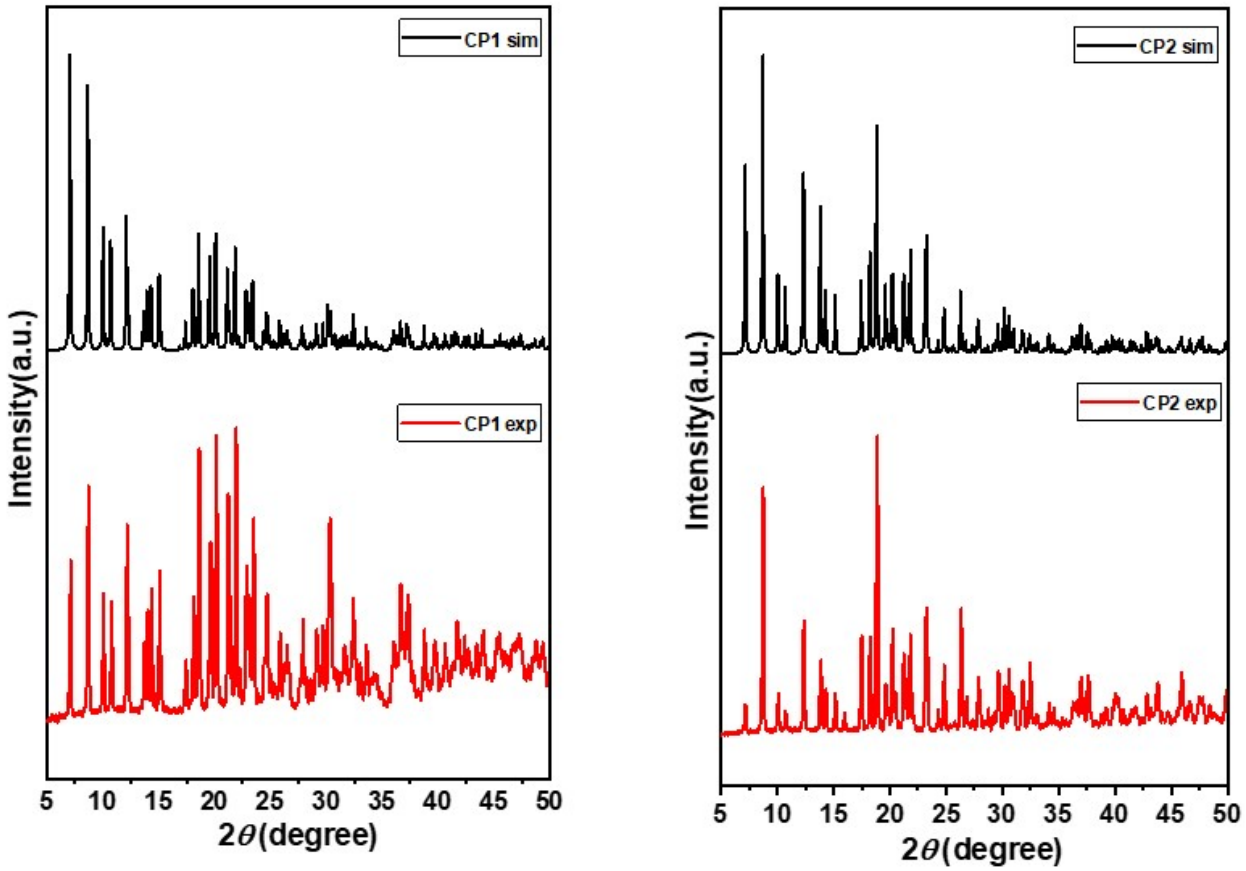

Fig. S16.1 Comparison of simulated and experimental PXRD patterns of **CP1** and **CP2**.

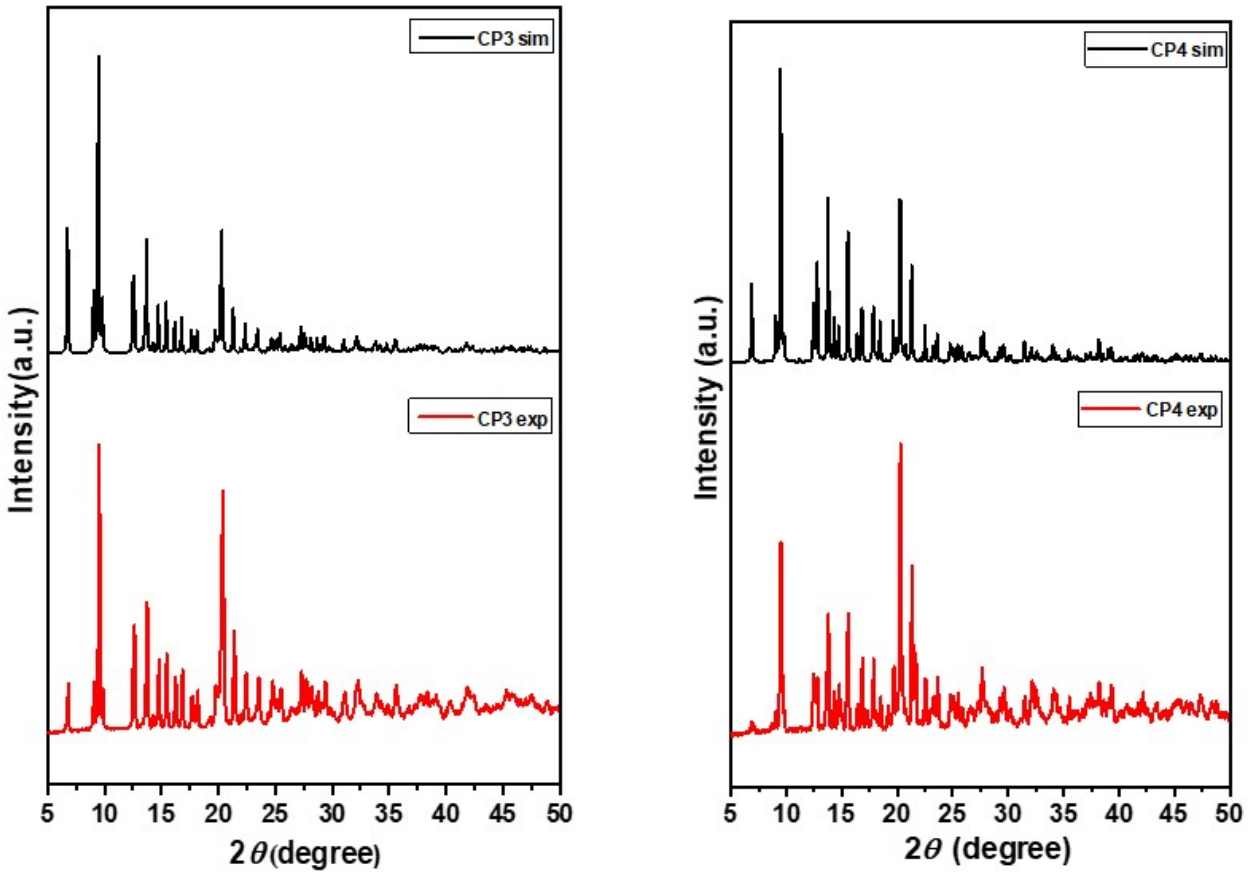

Fig. S16.2 Comparison of simulated and experimental PXRD patterns of **CP3** and **CP4**.

5.1. PXRD patterns of pristine and ground CPs

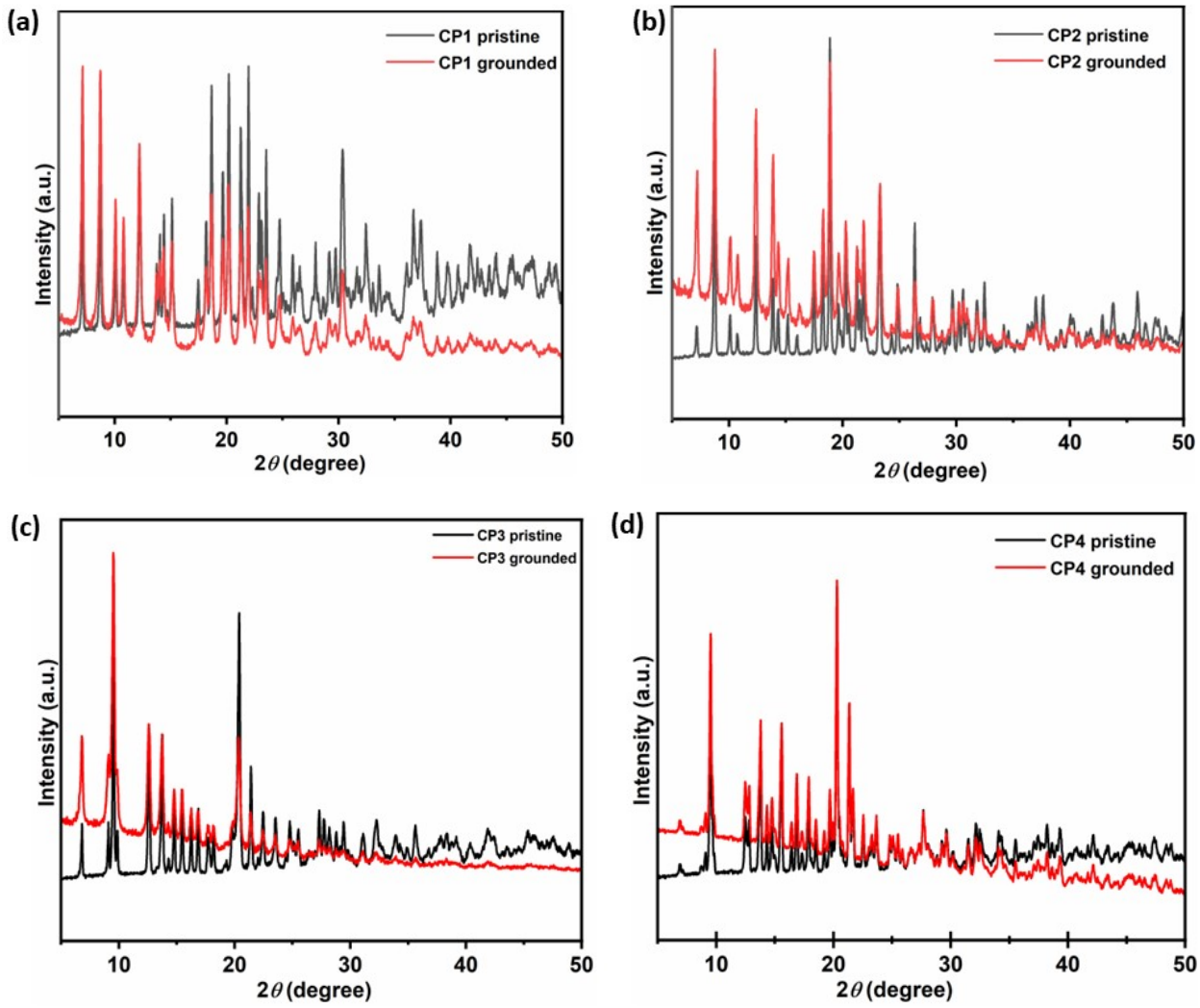

Fig. S17 PXRD patterns of pristine and ground CPs.

6. Thermogravimetric analysis (TGA) : Temperature gradient (TG) analyses experiments were performed in the range of 30–800 °C, using a heating rate of 10 °C min^{-1} under nitrogen flow. The thermogravimetric curves (shown in Figure S18) demonstrate that no solvent molecules are present in the CP's (1-4) structure. TGA performed on all the compounds confirms their stability up to 200 °C. It is reported that a slight increase in weight in the TGA curve between the temperature range 30-200 °C is observed due to the buoyancy effect. As the temperature increases, the density of the gas (fluid) decreases, resulting in a slight mass gain during the analysis. This effect is prominent in the lower temperature range; as the temperature increases, the buoyancy effect decreases.

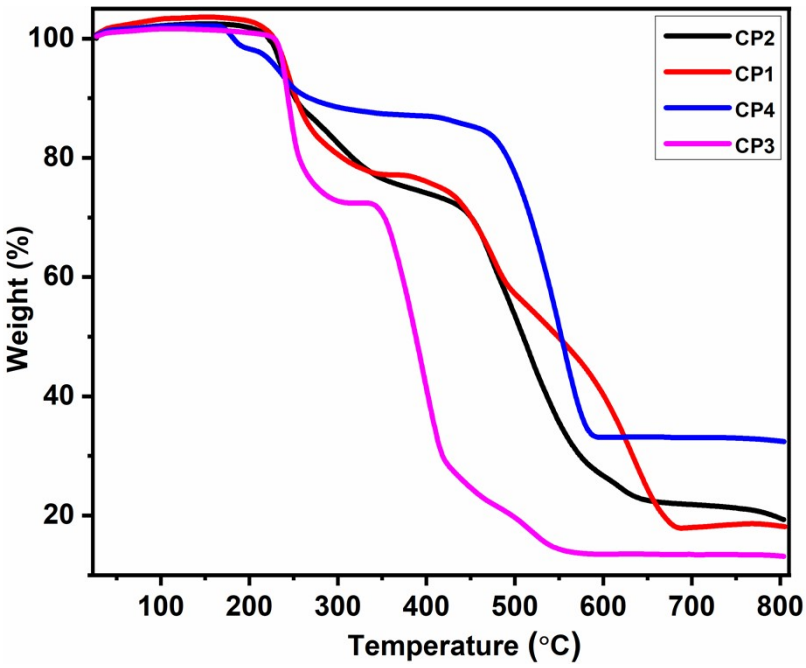

Fig.S18 TGA graph of **CP1**, **CP2**, **CP3**, and **CP4**.

7. TICT Phenomenon

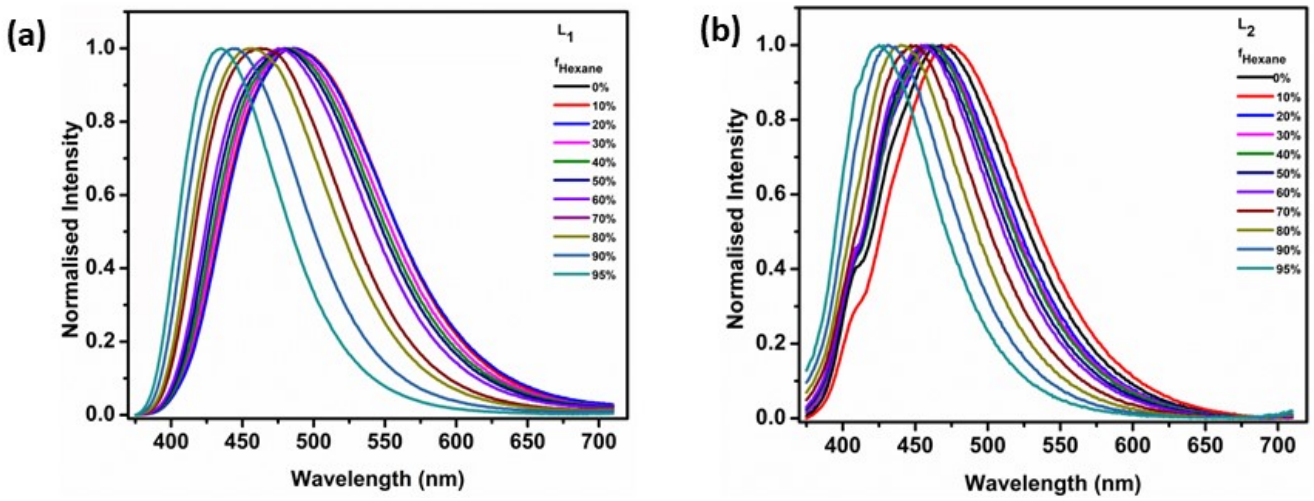

Fig. S19 Emission spectra of $\mathbf{L_1}$ (a) and (b) $\mathbf{L_2}$ in THF and THF/hexane mixtures (c = 1mM) with increasing fractions of hexane; formation of TICT state.

1. O. V. Dolomanov, L. J. Bourhis, R. J. Gildea, J. A. Howard and H. Puschmann, *Journal of applied crystallography*, 2009, **42**, 339-341.
2. G. M. Sheldrick and T. R. Schneider, in *Methods in enzymology*, Elsevier, 1997, vol. 277, pp. 319-343.